Interface Chemistry and Molecular Interactions of Phosphonic Acid Self-Assembled Monolayers on Oxyhydroxide-Covered Aluminum in Humid Environments

ARTICLE *in* LANGMUIR · MAY 2011

Impact Factor: 4.46 · DOI: 10.1021/la200445x · Source: PubMed

4 AUTHORS, INCLUDING:

Peter Thissen
Karlsruhe Institute of Technology
33 PUBLICATIONS **489** CITATIONS
SEE PROFILE

Miroslaw Giza
ThyssenKrupp AG
11 PUBLICATIONS **131** CITATIONS
SEE PROFILE

Langmuir

ARTICLE

pubs.acs.org/Langmuir

Interface Chemistry and Molecular Interactions of Phosphonic Acid Self-Assembled Monolayers on Oxyhydroxide-Covered Aluminum in Humid Environments

Michael Maxisch,[†] Peter Thissen,[†] Miroslaw Giza,[‡] and Guido Grundmeier*[,†]

[†]Department of Technical and Macromolecular Chemistry, University of Paderborn, Warburger Str. 100, 33098 Paderborn, Germany

[‡]ThyssenKrupp Steel Europe AG, Eberhardstrasse 12, 44145 Dortmund, Germany

ABSTRACT: Barrier properties of self-assembled octadecylphosphonic acid (ODPA) monolayers on plasma-modified oxyhydroxide-covered aluminum surfaces were analyzed by means of in situ photoelastic modulated infrared reflection absorption spectroscopy (PM-IRRAS). The surface hydroxyl density prior to ODPA adsorption was increased by means of a low-temperature H_2O-plasma treatment. Adsorption isotherms of H_2O on ODPA self-assembled monolayer (SAM) modified surfaces in comparison to bare oxide covered aluminum surfaces showed that the ODPA SAM leads to a strongly reduced amount of adsorbed water based on the inability of water to form hydrogen bonds to the low-energy aliphatic surface. However, the ODPA SAM covered surfaces did not show a significant inhibition of the H_2O/D_2O isotope exchange reaction between the D_2O gas phase and the hydroxyl groups of the aluminum oxyhydroxide film, as the interfacial layer between the ODPA SAM and the metal substrate, while the interfacial phosphonate group as well as the orientation of the SAM is not affected by the adsorption of water. It can be followed that the strong adhesion promoting and high corrosion resistances of organophosphonate monolayers on oxyhydroxide-covered aluminum is a result of the strong acid−base interaction of the phosphonate headgroup with the Al ions in the oxyhydroxide film, even in the presence of high interfacial water activity and the molecular interactions of the aliphatic chains. However, the barrier effect of such monolayers on the transport of water is negligible.

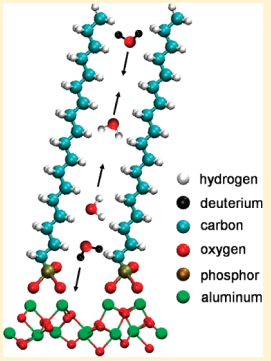

1. INTRODUCTION

The corrosion resistance and the adhesion of organic coatings and adhesives on oxyhydroxide-covered aluminum is of high importance and is mainly determined by the alloy composition, the surface chemistry of the alloy, and the composition of the polymeric film. To substitute traditional surface technologies, such as anodizing or conversion chemistry, adhesion-promoting, ultrathin films or even monomolecular layers like SAMs of organophosphonic acids have been investigated as new advanced interfacial layers for polymer-coated aluminum alloys.[1−6] Although the adhesion and interfacial corrosion protection of these adsorbed monolayers proved to be excellent, even in comparison to thicker conversion films, the barrier properties and the influence of water on the interface chemistry between the adsorbed organosphosphonic acid and the oxide-covered substrate were not evaluated in detail.

Alexander et al.[7] showed that an aluminum surface is covered by a thin pseudoboehmite layer under atmospheric conditions. This layer consists of the two main phases γ-Al_2O_3 and γ-AlOOH. The hydroxide to oxide ratio can be characterized by means of high-resolution X-ray photoelectron spectroscopy (XPS) and appropriate curve fitting. It was observed that surface hydroxyl groups promote the adsorption of organophosphonates and that the adhesion of the phosphonate group is based on an acid−base interaction. The driving force is assumed to be the formation of a surface salt, as already described for long-chain carboxylic acids by Allara et al.[8] and recently by Terryn et al.[9,10] Giza et al.[11] employed quartz crystal microweighing to investigate the effect of the surface hydroxylation on the adsorption rate of octadecylphosphonic acid (ODPA) on aluminum films. It was shown that the adsorption rate strongly depends on the hydroxyl density of the surface and can be directly influenced by a plasma modification of the oxyhydroxide film. Wapner et al.[1] applied water-soluble 1,3-aminopropylphosphonic acid (APPA) as short-chain adhesion-promoting molecules on aluminum alloy surfaces from dilute aqueous solutions and from a liquid adhesive film and showed excellent filiform corrosion resistance. Maege et al.[3] investigated the adsorption of amino-functionalized long-chain organophosphonic acids on pure aluminum substrates and have shown an equivalent corrosion protection and an improved adhesion to model coatings in comparison to chromated surfaces. Pahnke et al.[2] showed the effective coupling of benzophenone-containing organophosphonates to oxide-covered aluminum surfaces, which opens the way of adhesion promotion to organic layers via a photochemical reaction.

There have been many spectroscopic, microscopic, and theoretical studies of thin film interactions and molecular configurations at the bulk water/substrate interface.[12−15] However, the

Received: February 2, 2011
Revised: March 18, 2011
Published: April 13, 2011

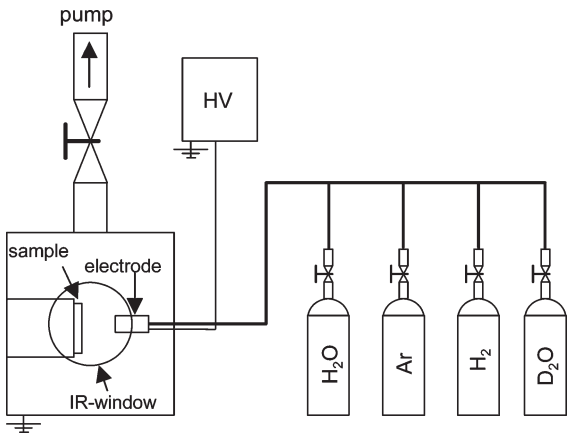

Figure 1. Schematic drawing of the experimental setup including plasma treatment and in situ PM-IRRAS.

microscopic details of how the water interacts with a polar surface covered with a hydrophobic monolayer is still not fully understood. Incorporation of water at the organic/oxide interface promotes wet delamination of organic layers which are bound to the surface via van der Waals (vdW) forces. It is of high interest to understand the origin of the high molecular adhesion forces of hydrophobic organophosphonate monolayers on oxide-covered surfaces, which might be based on the barrier properties for water or the water-resistant interfacial chemical bond.

Very recently, molecular interactions of ODPA with polar and unpolar single crystalline α-Al_2O_3 surfaces and amorphous Al-oxyhydroxide films were studied.[16] These studies show that the molecular adhesion of phosphonic acid groups depends on the interatomic distances between the surface Al ions and the polarity of the surfaces.

In the present studies, the D_2O adsorption from humid atmosphere on oxide-covered aluminum films and on SAMs of ODPA was analyzed by means of in situ photoelastic modulated infrared reflection absorption spectroscopy (PM-IRRAS) to spectroscopically study the barrier properties of self-assembled ODPA monolayers and the interface chemistry of the phosphonic acid groups in the presence of high water activities. Adsorption isotherms and isotope exchange reactions were measured to distinguish between the effects of surface energy, interfacial bonds, and barrier properties.

2. EXPERIMENTAL SECTION

2.1. Sample Preparation. Aluminum layers were deposited on silicon wafers [p-doped, Si(100), Si-Mat] by physical vapor deposition (PVD). The samples were coated with a 100 nm aluminum layer (Al 99.99%, Goodfellow GmbH) using thermal evaporation (Tectra GmbH). During the evaporation the layer thickness was monitored by a QCM (Tectra GmbH). Prior to film deposition the samples were thoroughly cleaned in a mixture of hydrogen peroxide (35%, Stockmeier Chemie GmbH & Co. KG) and ammonia (25%, Stockmeier Chemie GmbH & Co. KG) (1:1) for 60 min at 80 °C and afterward rinsed with deionized water and dried in a stream of nitrogen (5.0 by Air Liquid).

2.2. Surface Chemistry. The experimental setup for the plasma treatment and in situ PM-IRRAS is shown in Figure 1.

The vacuum cell includes two ZnSe windows to irradiate IR light from a spectrometer and one quartz glass window. The sample is placed vertically in the cell under a 80° geometry and fixed by a mask. Different sets of electrodes allow the generation of low-pressure remote and direct plasma. A commercial high-voltage power supply (G2000, Redline Technologies) was used to apply an alternating, pulsable, and adjustable voltage with a frequency of 36.1 kHz to one of the electrodes. In the case of direct plasma, the grounded sample functions as the second electrode. The base pressure of the chamber before flushing with the working gases was ensured to be in the range of 10^{-3} mbar. The pressure of the corresponding gas atmosphere during all plasma modifications was adjusted to 0.3 mbar. Pure gases argon and hydrogen were used for the experiments, in the quality 5.0 by Air Liquid. A closed flask with a high-precision valve was filled with ultrapure water (respectively D_2O) and was used for water (respectively D_2O) plasma modification. For the adjustment of the water (respectively D_2O) vapor atmosphere in the plasma chamber at 0.3 mbar, the water (D_2O) partial pressure was used and the pumping system was throttled.

2.3. Monolayer Preparation. The ODPA monolayers on plasma-modified aluminum were prepared by means of a self-assembly process from ethanolic solutions under ambient conditions. Substrates were immersed into a 1 mM ethanolic (>99.9%, Berkel AHK Alkoholhandel GmbH & Co. KG) solution of ODPA (Alpha Aesar GmbH & Co. KG) for 24 h. After rinsing with ethanol for 2 min, the samples were dried in a stream of pure nitrogen.

2.4. Surface Analysis. For adsorption studies and plasma surface treatment, the plasma chamber is attached to a Vertex V70 spectrometer (Bruker Optik GmbH, Germany) to allow in situ spectroscopic analysis of the aluminum surface by means of PM-IRRAS. For photoelastic modulation, the incident IR-beam was p-polarized at an aluminum wire grid, modulated at 50 kHz with a ZnSe photoelastic modulator (PMA50, Bruker Optik GmbH), and hits the sample at 80° relative to the substrate surface normal. Light reflected from the sample was focused with a ZnSe lens onto a cryogenic mercury cadmium telluride (MCT) detector.

During plasma modification, spectra were recorded with a resolution of 4 cm^{-1} and 1024 single scans. For water adsorption studies, a spectral resolution of 8 cm^{-1} and 1024 scans (512 scans in the case of measurements at 0.3 mbar of D_2O pressure) was used to improve the signal-to-noise ratio.

2.5. Adsorption Studies. For adsorption studies the plasma chamber was attached to a custom-made gas flow control system consisting of two mass flow controllers (Mass Stream, Bronkhorst Mättig GmbH), three gas-washing bottles, and one humidity sensor (HygroFlex, Rotronic Messgeräte GmbH). With this system, the humidity within the vacuum chamber can easily be set to a relative humidity (RH) of 2%−90% and kept constant in the range of ±0.1%.

Preliminary to every time-dependent adsorption experiment and measurement of the water adsorption isotherm, the sample was placed in the vacuum cell and exposed to a base pressure in the range of 10^{-3} mbar for 15 min. Subsequently, the chamber was purged with dry synthetic air for a further 15 min and a reference spectrum was recorded.

After the measurement of the reference spectrum, the humidity was increased to 75% and kept constant for time-dependent measurements. For the measurement of water adsorption isotherms, the humidity was stepwise increased from 10% to 80% RH.

3. RESULTS AND DISCUSSION

3.1. Plasma Modification of Passive Films. Native oxide aluminum grows according to the Cabrera−Mott mechanism.[17] During a plasma modification, adsorbed oxygen and hydroxide ions produced by electron-impact-induced chemistry at the interface between the oxide and the plasma volume induce a strong electric field across the oxide layer that drives ionic migration through the film. Depending on the specific mobility of the species, either aluminum ions move toward the oxide surface or oxygen ions toward the metal/oxide interface.

dx.doi.org/10.1021/la200445x |*Langmuir* 2011, 27, 6042–6048

Table 1. Relevant Parameters of the Different Plasma Treatment

gas composition	partial pressure/mbar	treatment time/s	plasma voltage/V
Ar/H_2	0.25/0.05	120	600
H_2O	0.3	120	600
D_2O	0.3	120	600

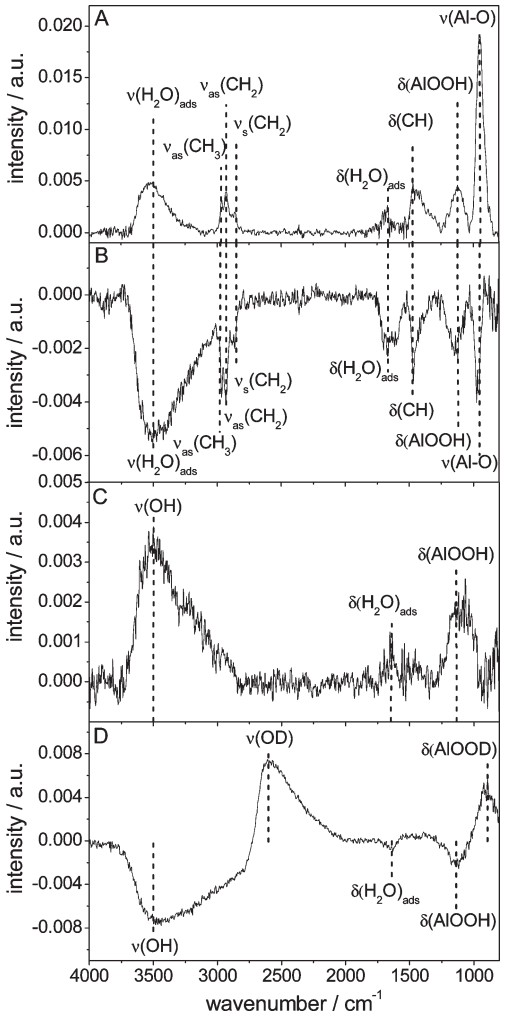

Figure 2. In-situ PM-IRRAS of an oxyhydroxide film covered aluminum surface (A) and after 120 s Ar/H_2-plasma cleaning (B) (with the bare substrate as background). In-situ PM-IRRAS of the cleaned oxide-covered aluminum surface after a 120 s H_2O-plasma modification (C) and after subsequent 120 s D_2O-plasma modification (D).

The transport of electrons is considered to be independent of the ionic motion and fast in comparison to the ion transport.[18]

To achieve a carbon contamination free surface, each sample was initially cleaned in an Ar/H_2-plasma. This cleaning step leads to a removal of residual organic contaminations and carbonates or organocarboxylates and a decrease of the amount of hydroxides within the native oxide layer.[19,11] In a second step, the hydroxyl density and the thickness of the oxyhydroxide layer was increased by means of H_2O-plasma.[11] All plasma-relevant parameters are presented in Table 1.

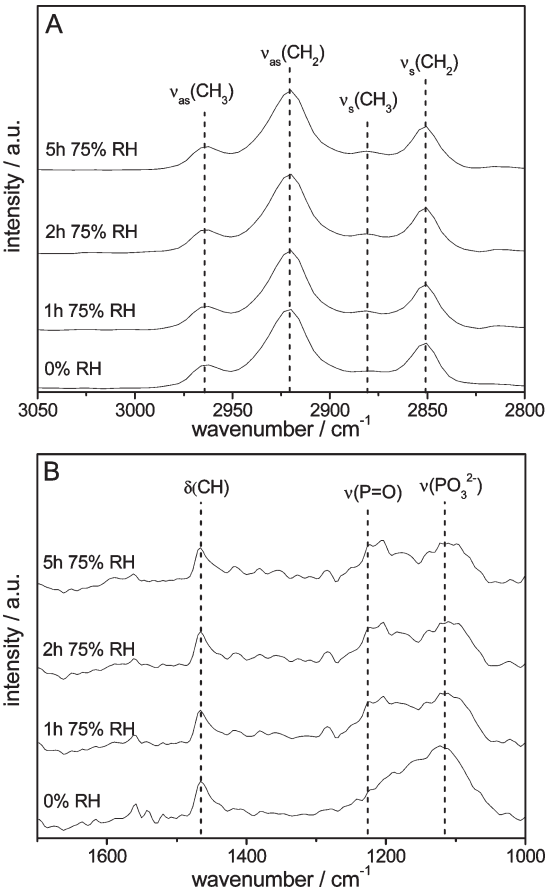

Figure 3. PM-IRRA spectra of an oxyhydroxide film covered aluminum surface after adsorption of an ODPA monolayer and during exposure to a humid atmosphere (75% RH) containing D_2O (The spectrum of the bare substrate was subtracted from each ODPA spectra). Part A shows the spectral region of CH_x vibration modes and part B shows the lower range of the spectra, including deformation vibration modes of CH and phosphonic acid signals.[3,11,21]

In Figure 2 the in situ PM-IRRAS data of an aluminum-coated silicon wafer surface before (A) and during plasma modification are shown. The difference spectrum of the surface after 120 s Ar/H_2-plasma treatment (B) shows negative peaks and thereby the removal of hydroxyls, adsorbed water, and organic contaminations. The in situ PM-IRRAS data after a subsequent H_2O-plasma treatment is presented in Figure 2 C. After the H_2O-plasma treatment, the surface is enriched in hydroxyl groups, as indicated by the positive peaks at 3500 cm^{-1} assigned to OH streching mode and 1115 cm^{-1} assigned to the AlOOH vibration mode. The latter peak increase can also hint at a slight increase in the passive film thickness due to the oxdiative plasma.[11]

The small positive peak at 1645 cm^{-1} assigned to the deformation vibration of adsorbed water indicates that after the water-plasma treatment more water molecules are adsorbed on the surface.

The spectrum after a subsequent D_2O-plasma modification is shown in Figure 2 D to illustrate the spectral change after complete exchange of protons. The isotopic proton exchange reaction is clearly reflected by the decrease in the OH peak intensity at 3500 cm^{-1} and the increase in the OD peak intensity at 2600 cm^{-1}.

The spectral region between 3700 and 2800 cm^{-1} includes the vibration modes of terminal hydroxyls, bridging hydroxyls,

dx.doi.org/10.1021/la200445x |*Langmuir* 2011, 27, 6042–6048

Table 2. List of Relevant Peak Positions and Intensities of ODPA during Exposure to 75% Relative Humidity of D_2O for 5 h

	$\nu_{as}(CH_3)$		$\nu_{as}(CH_2)$		$\nu_s(CH_3)$		$\nu_s(CH_2)$				
time/ min	position/ cm^{-1}	intensity/ au	position/ cm^{-1}	intensity/ au	position/ cm^{-1}	intensity/ au	position/ cm^{-1}	intensity/ au	azimuth angle/deg	δ(CH) intensity/ au (1465 cm^{-1})	PO_3^{2-} intensity/ au (1115 cm^{-1})
0	2962.4	0.0066	2919.9	0.0219	2879.2	0.0049	2850.5	0.0125	17.3	0.0058	0.0088
5	2961.7	0.0065	2920.3	0.0215	2880.8	0.0053	2850.8	0.0129	17.4	0.0053	0.0066
20	2961.7	0.0063	2919.7	0.0214	2880.8	0.0051	2850.8	0.0123	17.6	0.0053	0.0057
40	2962.3	0.0064	2920.3	0.0217	2881.4	0.0052	2850.8	0.0126	17.5	0.0053	0.0061
60	2961.7	0.0065	2920.3	0.0218	2881.4	0.0052	2850.8	0.0125	17.4	0.0052	0.0061
90	2961.7	0.0064	2919.7	0.0218	2881.4	0.0052	2850.8	0.0123	17.6	0.0055	0.0048
120	2961.7	0.0063	2920.9	0.0216	2880.8	0.0053	2850.8	0.0123	17.6	0.0055	0.0054
150	2962.4	0.0064	2920.3	0.0215	2880.8	0.0051	2850.8	0.0121	17.4	0.0053	0.0050
180	2962.4	0.0063	2920.3	0.0219	2881.4	0.0051	2050.8	0.0117	17.7	0.0052	0.0057
240	2962.4	0.0065	2920.3	0.0220	2880.8	0.0053	2050.8	0.0119	17.4	0.0055	0.0048
300	2962.4	0.0065	2920.3	0.0219	2880.2	0.0052	2850.8	0.0119	17.4	0.0055	0.0047

Table 3. List of Relevant Peak Positions and Intensities of ODPA during Exposure to D_2O Vapor (0.3 mbar) for 5 h

	$\nu_{as}(CH_3)$		$\nu_{as}(CH_2)$		$\nu_s(CH_3)$		$\nu_s(CH_2)$				
time/ min	position/ cm^{-1}	intensity/ au	position/ cm^{-1}	intensity/ au	position/ cm^{-1}	intensity/ au	position/ cm^{-1}	intensity/ au	azimuth angle/ deg	PO_3^{2-} position/ cm^{-1}	PO_3^{2-} intensity/ au
0	2966.1	0.0052	2923.8	0.0097	2877.5	0.0035	2854.1	0.0050	12.6	1116.7	0.0056
10	2965.9	0.0061	2923.7	0.0106	2877.3	0.0040	2853.9	0.0054	12.0	1112.2	0.0053
20	2966.3	0.0051	2923.6	0.0101	2877.3	0.0041	2853.9	0.0057	13.0	1111.5	0.0048
30	2966.6	0.0059	2923.6	0.0106	2877.6	0.0040	2853.9	0.0051	12.3	1114.5	0.0051
60	2965.8	0.0051	2923.9	0.0098	2877.5	0.0034	2854.1	0.0049	12.6	1106.3	0.0049
90	2966.1	0.0059	2923.7	0.0099	2877.7	0.0034	2854.0	0.0052	13.0	1113.7	0.0049
120	2966.3	0.0049	2923.6	0.0096	2877.4	0.0037	2854.5	0.0050	12.8	1110.8	0.0053
150	2966.2	0.0062	2923.5	0.0106	2877.4	0.0042	2854.3	0.0053	11.9	1107.8	0.0052
180	2966.2	0.0063	2923.8	0.0109	2877.8	0.0044	2854.3	0.0057	12.0	1118.2	0.0054
210	2966.3	0.0059	2923.6	0.0108	2878.0	0.0042	2854.0	0.0054	12.4	1103.3	0.0057
240	2966.1	0.0054	2923.9	0.0108	2877.4	0.0036	2854.2	0.0051	13.0	1107.0	0.0052
270	2966.4	0.0064	2923.5	0.0111	2877.5	0.0045	2854.2	0.0056	12.0	1121.9	0.0052
300	2966.2	0.0066	2923.8	0.0110	2877.5	0.0045	2854.1	0.0057	11.7	1110.8	0.0047

hydrogen-bonded hydroxyls, and water (3200−3500 cm^{-1}).[9] The fingerprint region between 800 and 1400 cm^{-1} shows that the protons of the AlOOH layer were exchanged by deuterium ions, leading to the formation of a AlOOD layer.[20]

3.2. PM-IRRAS Study of the ODPA SAM in D_2O Atmospheres. The adsorbed ODPA monolayers on oxide-covered aluminum were characterized before and during every adsorption study by means of in situ PM-IRRAS. In Figure 3 a selection of spectra obtained during the exposure of ODPA SAM covered aluminum at 75% relative humidity of D_2O is shown.

Part A shows the peaks of CH_2 and CH_3 vibration modes before and their evolution during exposure to 75% RH of D_2O. Part B includes the CH deformation vibration and the phosphonic acid signals. Peak intensities and positions are listed in Table 2 in detail. For the D_2O-adsorption at reduced pressure, a detailed list of peak intensities and positions is given in Table 3.

According to the literature, octadecylphosphonic acid forms self-assembled and ordered monolayers on oxide-covered aluminum surfaces.[3,11] A useful parameter to characterize the ordering of the monolayer is the position of the methylene stretching modes, which usually shift to higher frequencies with increasing conformational disorder of the alkyl chains.[22] It has been observed that an ordered aliphatic monolayer contains chains in all-trans configuration which are characterized by IR peak positions of $\nu_{as}(CH_2)$ smaller than 2920 cm^{-1} and $\nu_s(CH_2)$ smaller than 2850 cm^{-1}.[23−26] Therefore, it can be followed that ODPA has formed a well-ordered monolayer on oxide-covered aluminum under the here presented conditions.

To characterize the orientation of the monolayer, the ratio between CH_3 and CH_2 peak intensity can be utilized. For a perfectly rectangular adsorbed molecule no intensity would be expected for the CH_2 groups, because of the missing transition dipole moment in the direction normal to the investigated surface. A geometrical estimation for the calculation of the azimuth angle is[27]

$$\frac{I_{CH_2}}{I_{CH_3}} = \frac{2n \cdot \cos^2(90° - \alpha)}{3 \cdot \cos^2(35° - \alpha)}$$

where I_i is the intensity of the according CH valence vibration bands, n is the number of methylene groups in the alkyl chain, and α is the angle between the alkyl chain axis and the surface normal. These calculated azimuth angles are listed in Tables 2 and 3.

dx.doi.org/10.1021/la200445x |Langmuir 2011, 27, 6042–6048

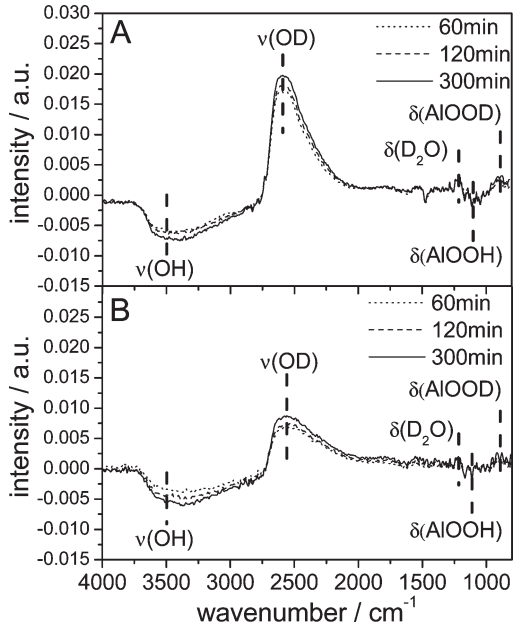

Figure 4. PM-IRRA difference spectra of oxyhydroxide-covered aluminum (A) and oxyhydroxide-covered aluminum with an adsorbed ODPA self-assembled monolayer (B) after exposure to a relative humidity of 75% in a D_2O atmosphere. Spectra were subtracted by the respective sample spectra in a dry atmosphere.

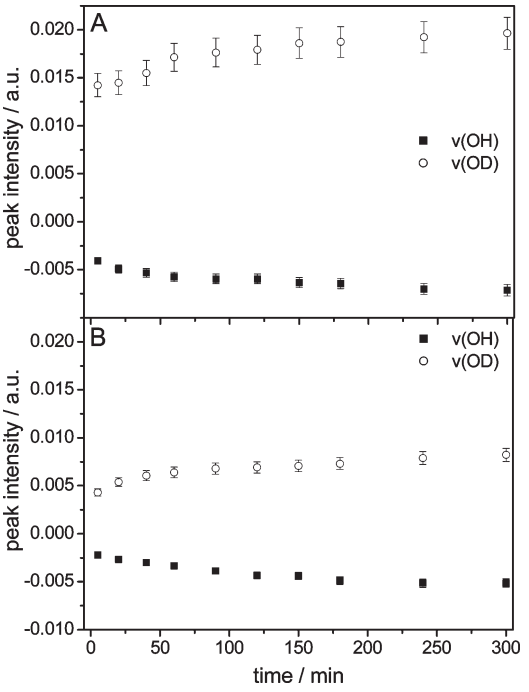

Figure 5. Illustration of the time-dependent change of OH and OD peak intensity of bare (A) and ODPA-coated surface (B) during exposure to 75% relative humidity of D_2O.

Prior to exposure to the humid environment, the corresponding tilt angle was 17.3° with respect to the surface normal.

After an increase of the relative humidity to 75% RH at ambient pressure, no significant change in the azimuth angle was observed. The azimuth angle of 17.5 ± 0.2° stayed constant over the time of exposure.

Moreover, no change in the peak positions of the asymmetric and symmetric stretching vibrations of the methylene and methyl groups were observed, indicating that no disorder takes place during adsorption of D_2O.

3.3. Proton Exchange Mechanisms and Kinetics during D_2O Adsorption. *3.3.1. Proton Exchange at Ambient Pressure.* Figures 4 and 5 show the comparison of the kinetics of D_2O adsorption as measured by means of in situ PM-IRRAS on oxyhydroxide-covered aluminum with and without an adsorbed ODPA SAM.

Prior to the measurements of the D_2O adsorption, the chamber was evacuated to 10^{-3} mbar for 15 min and purged with dry synthetic air, leading to a measured relative humidity of less than 2%. After the measurement of the reference spectrum, the relative humidity was increased to 75% and kept constant during the measurement.

The process can be assumed to consist of the following steps:

$$D_2O_{(g)} \rightarrow D_2O_{(ads,\ ODPA\ surface)}$$

$$D_2O_{(ads,\ ODPA\ surface)} \rightarrow D_2O_{(ads,\ ODPA/AlOOH\ interface)}$$

$$D_2O_{(ads,\ ODPA/AlOOH\ interface)} + 2AlOOH \rightarrow H_2O_{(ads,\ ODPA/AlOOH\ interface)} + 2AlOOD$$

$$H_2O_{(ads,\ ODPA/AlOOH\ interface)} \rightarrow H_2O_{(ads,\ ODPA\ surface)}$$

$$H_2O_{(ads,\ ODPA\ surface)} \rightarrow H_2O_{(g)}$$

Figure 4 A shows the resulting PM-IRRA difference spectra as recorded for the bare oxyhydroxide-covered aluminum sample. As the two relevant processes, the adsorption of D_2O mono- or multilayer and the isotopic proton exchange within the oxyhydroxide layer take place. The exchange of protons is indicated by a reduction of peak intensity at 3500 and 1115 cm^{-1}, assigned to the OH and AlOOH vibration modes, and the simultaneous increase in peak intensity at 2600 and 886 cm^{-1}, assigned to OD and AlOOD vibration modes.[20]

Moreover, the intensity of the arising OD peak was observed to be larger than the negative OH peak. In combination with the recorded signal for the D_2O deformation vibration (1200 cm^{-1}), a formation of a D_2O layer can be assumed.

An illustration of the evolution of OH and OD peaks is shown in Figure 5 A. After a strong initial change, the positive and negative peak intensities reached a limiting value.

Very similar results were observed for the ODPA-covered oxyhydroxide surface (Figures 4 B and Figure 5 B). However, in the case of the adsorbed ODPA SAM, the OH and OD peak intensities were observed to be smaller, indicating mainly a reduction in adsorbed D_2O equilibrium layer thickness. However, the kinetics of the proton exchange reaction was not significantly slowed down.

3.3.2. Proton Exchange at Reduced Pressure. In order to study the proton exchange kinetics without the parallel formation of an adsorbed multilayer water film, a similar study was performed under reduced D_2O partial pressure of 0.3 mbar.[28]

In Figure 6, the observed difference spectra are shown. The comparison of the development of the OD and OH peak intensities is shown in Figure 7.

Since no D_2O deformation vibration modes were detected, it can be assumed that for both surfaces at 0.3 mbar D_2O the approximate amount of 0.5 monolayers[29] of water was below the detection limit and that the isotopic proton exchange reaction dominated the spectra.

dx.doi.org/10.1021/la200445x |*Langmuir* 2011, 27, 6042–6048

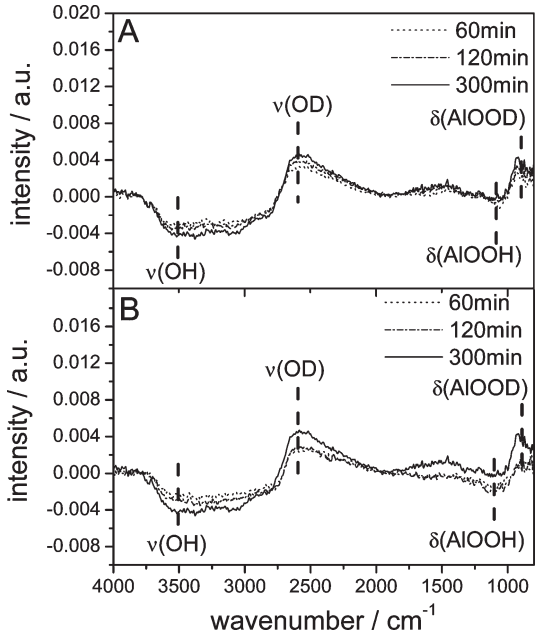

Figure 6. PM-IRRA difference spectra of oxyhydroxide-covered aluminum (A) and oxyhydroxide-covered aluminum with an adsorbed ODPA SAM (B) during exposure to D_2O vapor at 0.3 mbar pressure. Spectra were subtracted by the respective sample spectra under an argon atmosphere (0.3 mbar).

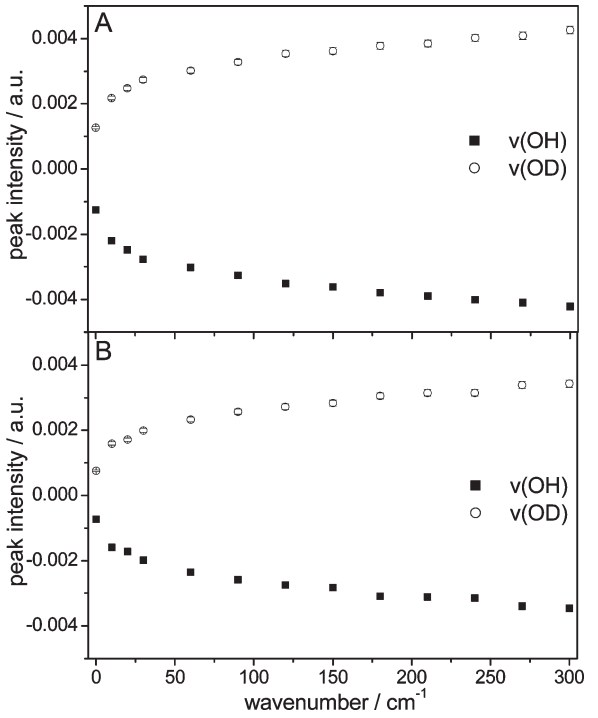

Figure 7. Illustration of the time-dependent change of OH and OD peak intensity of bare (A) and ODPA-coated surface (B) during exposure to D_2O vapor (0.3 mbar).

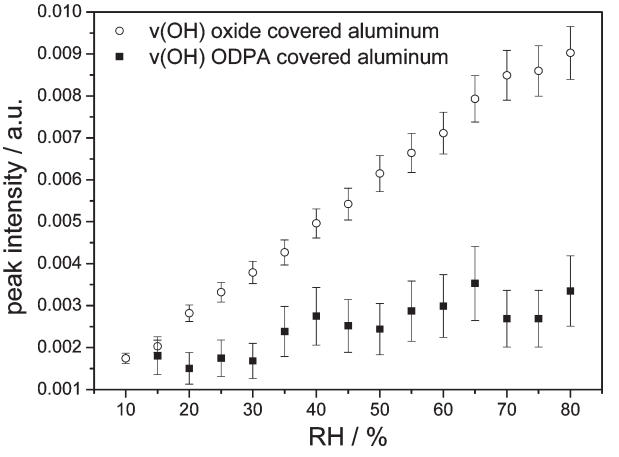

Figure 8. Illustration of the adsorption isotherms of H_2O on an oxide-covered aluminum surface and a surface covered with an ODPA SAM.

For the adsorption at 0.3 mbar, the difference in the observed spectra illustrating the proton exchange was even less for the two surface chemistries than in the case of the ambient pressure. The ODPA SAM did not significantly inhibit the isotopic proton exchange reaction, considering that the exact hydroxyl amount after the adsorption of ODPA on the surface is not well-known. At least only a little delay in the isotopic proton exchange reaction was observed. However, the constant signals and peak positions of the CH and phosphonate peaks (see Table 3) show that D_2O adsorption and isotopic exchange reactions do not lead to any change in the ordering or the interfacial binding of the organophosphonate SAM.

Thus, the rate-determining step in the overall proton exchange reaction is not the transport of D_2O molecules through the monolayer but the chemical reaction within the oxyhydroxide films.

3.4. Measurement of a Water Adsorption Isotherm. Figure 8 shows the comparison of the adsorption isotherms of H_2O measured by means of PM-IRRAS on oxyhydroxide-covered aluminum and on oxyhydroxide-covered aluminum with an adsorbed ODPA SAM.

Prior to the measurements, the chamber was purged with dry air, leading to a measured relative humidity of less than 2%. After the measurement of a reference spectrum, the relative humidity was increased step by step from 10% to 80%, and spectroscopic measurements were done for each step.

For the bare surface an almost linear increase of OH peak intensity was found over the range of studied relative humidity. In the case of an ODPA-covered surface, a significantly smaller increase of the OH peak intensity was observed. The reasons for the reduced adsorption of H_2O are the strongly reduced interaction energies between H_2O and the CH_3-terminated ODPA SAM. No hydrogen bonds as in the case of the oxyhydroxide-covered aluminum surface can be formed in this case.

4. CONCLUSIONS

Well-ordered ODPA SAMs could be adsorbed on plasma-activated passive-film-covered Al-surfaces. The corresponding PM-IRRAS data of the ODPA SAMs showed the characteristic peak for a deprotonated phosphonate group. The missing P−O−H stretching modes and the presence of the PO_3^{2-} stretching mode at 1115 cm^{-1} in the spectrum indicate formation of a bidentate binding to the amorphous oxide surface.[16]

During the adsorption of water no changes in the interfacial binding mechanism and the ordering of the alkyl chains were observed, as proven by in situ PM-IRRAS measurements. The in situ PM-IRRAS measurements allowed a detailed evaluation of

dx.doi.org/10.1021/la200445x |*Langmuir* 2011, 27, 6042–6048

the barrier properties of ODPA SAMs and the influence on the H_2O adsorption isotherm. Both aspects are of high relevance for adhesion phenomena related to organophosphonates.

Concerning the amount of water that is adsorbed on the surface, PM-IRRAS measurements revealed a significant decrease of the slope of the H_2O adsorption isotherms on oxide-covered aluminum induced by the adsorbed ODPA SAM. This behavior could be explained by the low surface energy of the well-ordered ODPA film and the negligible polar component of its surface energy. In situ PM-IRRAS measurements proved the self-assembly of the ODPA monolayer.

However, it could be shown that a proton exchange occurs within the AlOOH layer at the interface between the ODPA SAM and the Al metal substrate. The kinetics of this process are similar to those for the uncovered passive-film-coated Al substrate.

However, even though the interfacial water activity is increased in the neighborhood of the adsorbed phosphonate headgroup, no protonation and no desorption of the phosphonate group was observed. This proves that the stability of organophosphonates on oxide-covered aluminum surfaces is based on the high interfacial bond strength based on the bidentate binding and on the molecular van der Waals interactions of the alkyl chains, but not on the barrier properties of the film.

AUTHOR INFORMATION

Corresponding Author

*E-mail: g.grundmeier@tc.uni-paderborn.de.

ACKNOWLEDGMENT

The financial support of Bundesministerium für Bildung und Forschung (BMBF) is gratefully acknowledged. Peter Thissen gratefully acknowledges the financial support of the Deutsche Forschungsgemeinschaft (DFG). We also acknowledge the Theoretical and Computational Biophysics Group in the Beckman Institute for Advanced Science and Technology at the University of Illinois for providing the VMD software.[30]

REFERENCES

(1) Wapner, K.; Stratmann, M.; Grundmeier, G. *Int. J. Adhes. Adhes.* **2007**, *28*, 59–70.

(2) Pahnke, J.; Rühe, J. *Macromol. Rapid Commun.* **2004**, *25*, 1396–1401.

(3) Maege, I.; Jaehne, E.; Henke, A.; Adler, H. J. P.; Bram, C.; Jung, C.; Stratmann, M. *Prog. Org. Coat.* **1998**, *34*, 1–12.

(4) Jaehne, E.; Oberoi, S.; Adler, H. J. P. *Prog. Org. Coat.* **2008**, *61*, 211–223.

(5) Grundmeier, G.; Schmidt, W.; Stratmann, M. *Electrochim. Acta* **2000**, *45*, 2515–2533.

(6) Rohwerder, M.; Grundmeier, G.; Stratmann, M. Corrosion Protection by organic monolayers and thin polymer films. In *Corrosion Mechanisms in Theory and Practice*, 2nd ed.; Marcus, J. O. P, Ed.; CRC Press: New York, 2002; pp 479−527.

(7) Alexander, M. R.; Thompson, G. E.; Beamson, G. *Surf. Interface Anal.* **2000**, *29*, 468–477.

(8) Allara, D. L.; Nuzzo, R. G. *Langmuir* **1985**, *1*, 52–66.

(9) van den Brand, J.; Blajiev, O.; Beentjes, P. C. J.; Terryn, H.; de Wit, J. H. W. *Langmuir* **2004**, *20*, 6308–6317.

(10) van den Brand, J.; Blajiev, O.; Beentjes, P. C. J.; Terryn, H.; de Wit, J. H. W. *Langmuir* **2004**, *20*, 6318–6326.

(11) Giza, M.; Thissen, P.; Grundmeier, G. *Langmuir* **2008**, *24*, 8688–8694.

(12) Beaglehole, D.; Christenson, H. K. *J. Phys. Chem.* **1992**, *96*, 3395–3403.

(13) Hasegawa, T.; Nishijo, J.; Imae, T.; Huo, Q.; Leblanc, R. M. *J. Phys. Chem. B* **2001**, *105*, 12056–12060.

(14) Ewing, G. E. *J. Phys. Chem. B* **2004**, *108*, 15953–15961.

(15) Thissen, P.; Grundmeier, G.; Wippermann, S.; Schmidt, W. G. *Phys. Rev. B* **2009**, *80*, 25403.

(16) Thissen, P.; Valtiner, M.; Grundmeier, G. *Langmuir* **2010**, *26*, 156–164.

(17) Cabrera, N.; Mott, N. F. *Rep. Prog. Phys.* **1948**, *12*, 163–184.

(18) Stella, K.; Diesing, D. *J. Electrochem. Soc.* **2007**, *154*, C663–C670.

(19) Bertrand, N.; Bulkin, P.; Drévillon, B.; Lucas, S.; Benayoun, S. *Surf. Coat. Technol.* **1997**, *94−95*, 362–367.

(20) Kiss, A. B; Keresztury, G.; Farkas, L. *Spectrochimi. Acta, Part A* **1980**, *36*, 653–658.

(21) Maxisch, M.; Ebbert, C.; Torun, B.; Fink, N.; de los Arcos, T.; Lackmann, J.; Maier, H. J.; Grundmeier, G. *Appl. Surf. Sci.* **2011**, *257*, 2011–2018.

(22) Spori, D. M.; Venkataraman, N. V.; Tosatti, S. G. P.; Durmaz, F.; Spencer, N. D.; Zürcher, S. *Langmuir* **2007**, *23*, 8053–8060.

(23) Nuzzo, R. G.; Dubois, L. H.; Allara, D. L. *J. Am. Chem. Soc.* **1990**, *112*, 558–569.

(24) Quinones, R.; Gawalt, E. S. *Langmuir* **2007**, *23*, 10123–10130.

(25) Byrd, H.; Pike, J. K.; Talham, D. R. *Chem. Mater.* **1993**, *5*, 709–715.

(26) Porter, M. D.; Bright, T. B.; Allara, D. L.; Chidsey, C. E. D. *J. Am. Chem. Soc.* **1987**, *109*, 3559–3568.

(27) Bram, C.; Jung, C.; Stratmann, M. *Fresenius J. Anal. Chem.* **1997**, *358*, 108–111.

(28) Al-Abadleh, H. A.; Grassian, V. H. *Langmuir* **2003**, *19*, 341–347.

(29) Yamamoto, S.; Kendelewicz, T.; Newberg, J. T.; Ketteler, G.; Starr, D. E.; Mysak, E. R.; Andersson, K. J.; Ogasawara, H.; Bluhm, H.; Salmeron, M.; Brown, G. E.; Nilsson, A. *J. Phys. Chem. C* **2010**, *114*, 2256–2266.

(30) Humphey, W.; Dalke, A.; Schulten, K. VMD—Visual molecular dynamics. *J. Mol. Graphics* **1996**, *14.1*, 33–38.